Journal of Hydrology 404 (2011) 13–29

Contents lists available at ScienceDirect

Journal of Hydrology

journal homepage: www.elsevier.com/locate/jhydrol

Height Above the Nearest Drainage – a hydrologically relevant new terrain model

A.D. Nobre [a,b,*], L.A. Cuartas [b], M. Hodnett [c], C.D. Rennó [b], G. Rodrigues [b], A. Silveira [b], M. Waterloo [c], S. Saleska [d]

[a] Instituto Nacional de Pesquisas da Amazonia, Escritório Regional no INPE, Av. dos Astronautas, 1758, 12227-010 São José dos Campos/SP, Brazil
[b] Centro de Ciência do Sistema Terrestre/CCST, Instituto Nacional de Pesquisas Espaciais/INPE, Av. Dos Astronautas, 1758, 12227-010 Saão José dos Campos/SP, Brazil
[c] Department of Hydrology and Geo-environmental Sciences, Faculty of Earth and Life Sciences, Vrije Universiteit, De Boelelaan 1085, 1081 HV Amsterdam, The Netherlands
[d] Department of Ecology and Evolutionary Biology, University of Arizona, Tucson, AZ 85721, USA

ARTICLE INFO

Article history:
Received 13 July 2010
Received in revised form 27 January 2011
Accepted 24 March 2011
Available online 12 April 2011
This manuscript was handled by P. Baveye, Editor-in-Chief

Keywords:
Relative height
Normalization of topography
Gravitational potential
Draining potential
Flow path
Drainage network

SUMMARY

This paper introduces a new terrain model named HAND, and reports on the calibration and validation of landscape classes representing soil environments in Amazonia, which were derived using it. The HAND model normalizes topography according to the local relative heights found along the drainage network, and in this way, presents the topology of the relative soil gravitational potentials, or local draining potentials. The HAND model has been demonstrated to show a high correlation with the depth of the water table, providing an accurate spatial representation of soil water environments. Normalized draining potentials can be classified according to the relative vertical flowpath-distances to the nearest drainages, defining classes of soil water environments. These classes have been shown to be comparable and have verifiable and reproducible hydrological significance across the studied catchment and for surrounding ungauged catchments. The robust validation of this model over an area of 18,000 km^2 in the lower Rio Negro catchment has demonstrated its capacity to map expansive environments using only remotely acquired topography data as inputs. The classified HAND model has also preliminarily demonstrated robustness when applied to ungauged catchments elsewhere with contrasting geologies, geomorphologies and soil types. The HAND model and the derived soil water maps can help to advance physically based hydrological models and be applied to a host of disciplines that focus on soil moisture and ground water dynamics. As an original assessment of soil water in the landscape, the HAND model explores the synergy between digital topography data and terrain modeling, presenting an opportunity for solving many difficult problems in hydrology.

1. Introduction

Soil water has been extensively recognized as key parameter in conditioning landscape ecology and, therefore, in regulating land–atmosphere interactions (e.g. Turner, 1989; Entekhabi et al., 1996; Rodriguez-Iturbe, 2000). Elevation is a primary landscape attribute and a fundamental physical parameter defining soil–water gravitational potential energy (Moore et al., 1993). The characteristic water dynamics found on land are conditioned by physical features emerging from the interplay of elevation with geological substrates. Spatial variation of elevations results in gradients of potential energy, which become the main physical driver of water flows on and through emerse terrain, as well as within drainage channels. Digital Elevation Models (DEM) allow us to make calculations to describe, understand and predict water storage and movements on land (Moore et al., 1992). The quantitative analysis of DEMs has led to the development of a number of hydrologically relevant numerical descriptors of landscapes such as catchment area, flow path, accumulated contributing area and drainage networks (e.g. Tarboton, 1997; Curkendall et al., 2003). These topographic descriptors have revolutionized hydrologic modeling (Kalma and Sivapalan, 1995), leading to a growing number of bottom-up distributed physically based models (e.g. TOPOG, O'Loughlin, 1986; SHE, Abbott et al., 1986; IHDM, Beven et al., 1987; DHSVM, Wigmosta et al., 1994; OBJTOP, Wang et al., 2005). These models can simulate hydrological processes at the surface reasonably well and are better suited than lumped conceptual models for the prediction of future hydrological conditions due to climate and land use changes (Wigmosta et al., 2002). However, this advantage over lumped conceptual models (e.g. Wagener et al., 2004; Wagener and Wheater, 2006) has its drawbacks. Distributed physically based models require appropriate parameterization for watershed physical properties, rendering them as difficult to generalize to diverse unknown catchments as the rainfall/runoff models for ungauged catchments (e.g. Beven, 1996).

* Corresponding author at: Instituto Nacional de Pesquisas da Amazônia/ INPA, escritório regional no INPE, Av. Astronautas, 12227-010 São José dos Campos/SP, Brazil. Tel.: +55 12 3208 6737; fax: +55 12 3208 7130.

E-mail address: anobre27@gmail.com (A.D. Nobre).

0022-1694/$ - see front matter © 2011 Elsevier B.V. All rights reserved.
doi:10.1016/j.jhydrol.2011.03.051

In spite of this shortcoming, if parameter calibration could somehow be solved for large areas, the capacity to produce a generalized deterministic treatment of surface water dynamics could represent a great advance. Ideally, it would be convenient to use a hydrological model capable of representing the physical processes at one point, on a hill slope or in a small representative area where parameters may be measurable and have a clear physical meaning. Then, using a combination of surface attributes with the structure of the basin (Band and Moore, 1995) or as a regionalization method for transferring information (Flügel, 1995), the behavior in each unit would be aggregated to larger scales. However, a satisfactory (and consensual) methodology has not been developed that allows aggregation of processes on hillslopes and in representative areas (Beven, 1995; Schaake et al., 1996; Sivapalan et al., 2003a,b). Moreover, the integration in time and space of the equations governing the specific hydrological processes demands much information about the three-dimensional heterogeneity of surface geophysical attributes. This information is only available for a few small catchments, limiting the application of such methodology.

Topography has long been known to correlate with soil properties (e.g. Jenny, 1941; Gessler et al., 2000; Hansen et al., 2009) and is recognized as imposing strong controls on soil moisture and ground water dynamics (e.g. Beven and Kirkby, 1979; O'Loughlin, 1986, 1990; Haitjema and Mitchell-Bruker, 2005; Grabs et al., 2009). Superficial soil moisture conditions define the partitioning and destination of incoming and outgoing water fluxes both in space and time. Spatial patterns of soil moisture induced by topography play important roles in controlling infiltration-recharge/runoff (e.g. Dahl et al., 2007). Zones of convergent flow (concave and low-lying areas, such as valley floors) are typically zones of high soil moisture content. Higher areas in the landscape tend to be

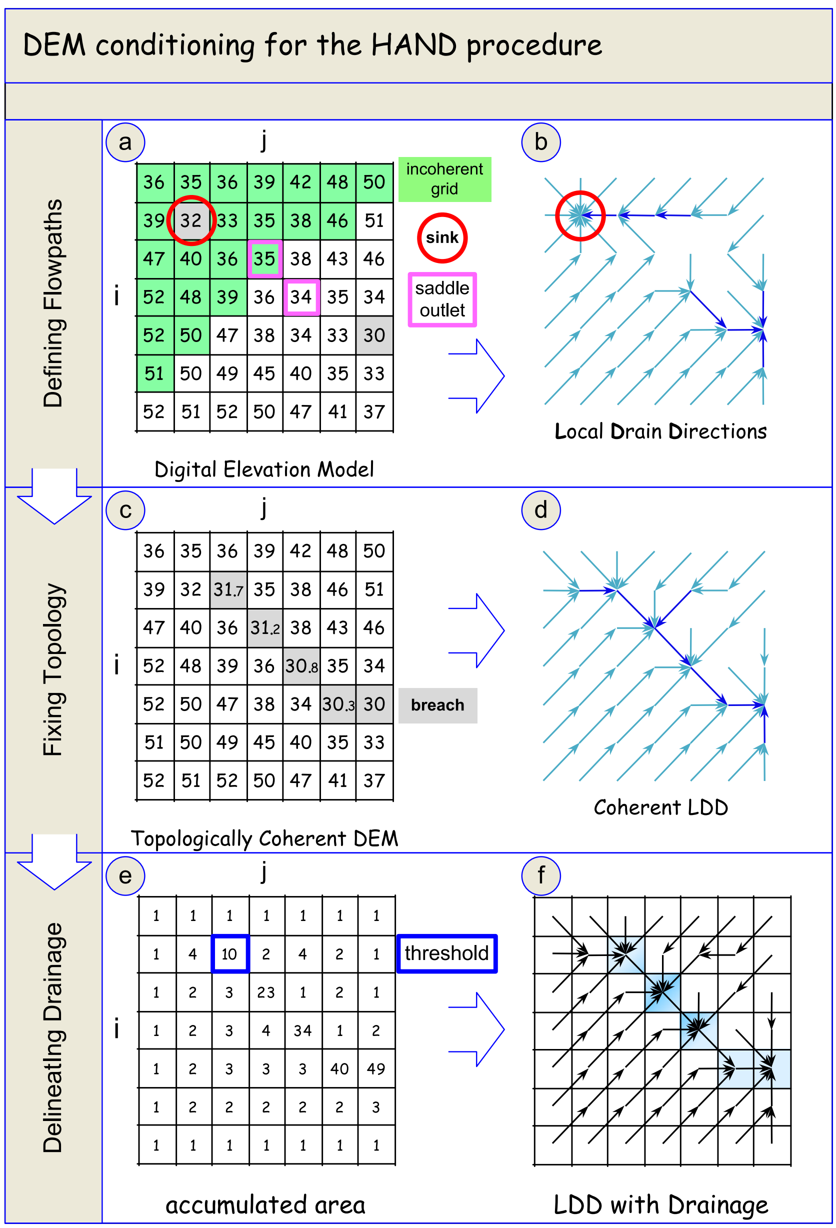

Fig. 1. Preliminary procedures required for HAND computations: (a) a DEM with sinks and partially incoherent hydrological topology is used as the source topography; (b) a network of flow pathways is defined from the local drain direction grid (LDD), generated using the D8 approach; (c) sinks are resolved through depression breaching, which then (d) allows for the topological correction of the LDD; (e) an accumulated area grid is generated by computing the total upslope area accumulated in each cell belonging to downhill directions, defined respectively by the LDD; and (f) a threshold value is found for the accumulated area that corresponds to the channel initiation (stream heads), thus defining the drainage network.

progressively drier (Stieglitz et al., 1997, Famiglietti et al., 1998). There have been a large number of analytical treatments for topography, which attempted to find relevant local physical properties, generalizable to the landscape (e.g. O'Loughlin, 1986; Moore et al., 1993; Thompson et al., 1997; Gessler et al., 2000; Hjerdt et al., 2004; Lindsay, 2005; Deng, 2007; Miliaresis, 2008). The topographic index for example, also known as the topographic wetness index (TWI, Beven and Kirkby, 1979), has been widely investigated as a topographical descriptor of soil water conditions (e.g. Sørensen et al., 2005; Grabs et al., 2009). However, to our knowledge, no landscape-scale normalization of topography, with relevance to the understanding of soil water dynamics, has been attempted. We aimed at developing a model able to make contrasting catchments, at the hillslope flowpath level, uniformly comparable. In this paper we present a new terrain model called *Height Above the Nearest Drainage* (HAND) that normalizes DEMs according to distributed vertical distances relative to the drainage channels. We classified the HAND model according to soil environments and calibrated the classes for the Asu catchment (Waterloo et al., 2006; Cuartas et al., 2007; Tomasella et al., 2008), mapping soil environments at its small scale (13 km^2). Finally we validated those HAND classes for a larger encompassing region in the lower Rio Negro region of central Amazonia, mapping soil environments at two additional scales (500 km^2 and 18,000 km^2).

2. The HAND model

The HAND model normalizes the topography in respect to the drainage network through two sets of procedures on a DEM. First, it runs a sequence of computations to create a hydrologically coherent DEM, define flow paths and delineate the drainage channels (Fig. 1). The correct definition of the stream network is key to the HAND procedure because the elevations of the drainage channel system are used to calculate the normalized terrain heights. Depressions in the DEM data can interfere with the determination of flow directions (e.g. Jenson and Domingue, 1988; Grimaldi et al., 2007). There are a number of well-experimented approaches for dealing with DEM depressions (e.g. O'Callagham and Mark, 1984, Garbrecht and Martz, 1997; Martz and Garbrecht, 1998; Jones, 2002). We picked the breaching method because it fares better for areas with moderate relief (Rieger, 1998; Jones, 2002; Lindsay and Creed, 2005). Flat surfaces in the DEM data can generate uncertainty in the determination of flow directions (Garbrecht and Martz, 1997; Nardi et al., 2008). However, this problem has little consequence for the HAND procedure because horizontal oscillation of a flowpath on a flat surface has no effect on the relative vertical position of surrounding terrain. The flow path network, adjusted to reflect the coherent topology, is the source data for the definition of the drainage network through channel initiation, set by an accumulated area threshold (O'Callaghan and Mark, 1984; Tarboton, 1997). According to Lindsay (2006) this is the most robust method for channel mapping.

The second and original set of procedures uses local drain directions and the drainage network to generate a nearest drainage map, which will ultimately guide the HAND operator spatially in the production of the normalized topology of the HAND model (Fig. 2). A detailed description of the algorithm was presented in Rennó et al. (2008).

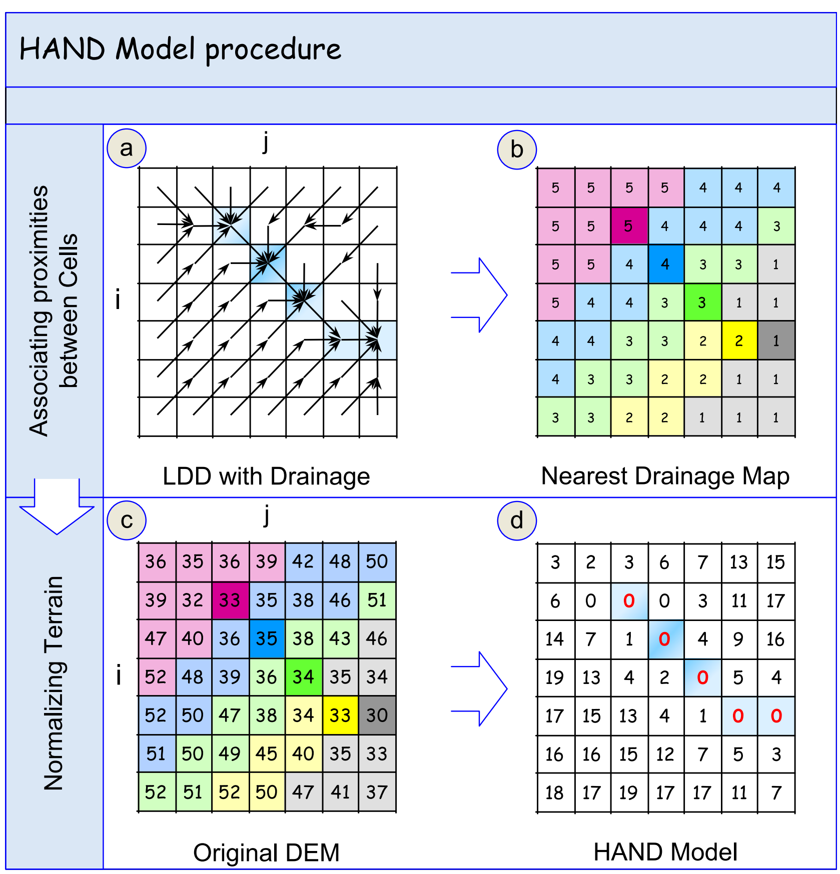

Fig. 2. Procedure to generate a HAND model: (a) the coherent LDD with the drainage network is used in the generation of (b) a nearest drainage map (each drainage cell is associated spatially with all DEM cells draining into it); then (c) the original DEM is processed using the HAND operator (the height of the corresponding drainage-outlet DEM cell is subtracted from the height of each hillslope DEM cell) and the nearest drainage map (which guides the operator, indicating the subtraction cell pairs), resulting in (d) the HAND model, where each cell height represents the difference in level to its respective nearest drainage cell. The drainage network is now converted into a normalized topographic reference so that the HAND model no longer retains a reference to sea level.

3. Finding significant HAND classes

Based on the normalized distribution of relative gravitational potentials, we report here the quantitative capacity of the HAND model to reveal and predict hydrologically relevant soil environments. The HAND model output of normalized heights is classified into HAND classes, which are defined based on field data or knowledge of local terrain, thus generating maps of soil environments (Fig. 3).

3.1. Study site and methods

The calibration and validation of the HAND classes were done in a large area in central Amazonia (Fig. 4, area (a) for calibration, and areas (b) and (c) for validation) with sites to the east of Rio Negro (Cuieiras and the adjacent Tarumã catchments) and to the west (Novo Airão). Calibration of HAND classes was done in the Igarapé Asu watershed, which is a third-order catchment (13.1 km^2) in a pristine rainforest nested within the larger study area (Fig. 5).

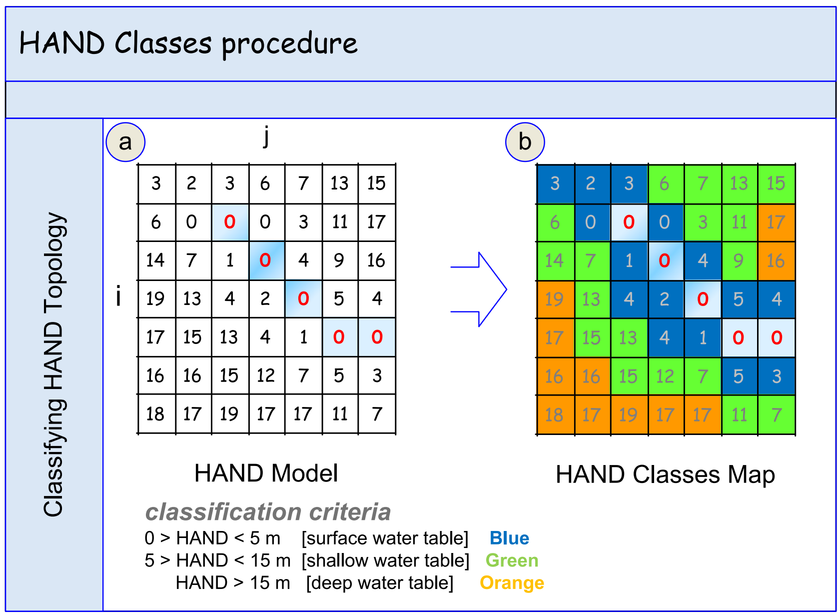

Fig. 3. Procedure to generate a HAND map of environments: (a) applying onto the HAND model a classification criteria, with the range of heights in each terrain class defined by the map's purpose, results in (b) a HAND map of environments.

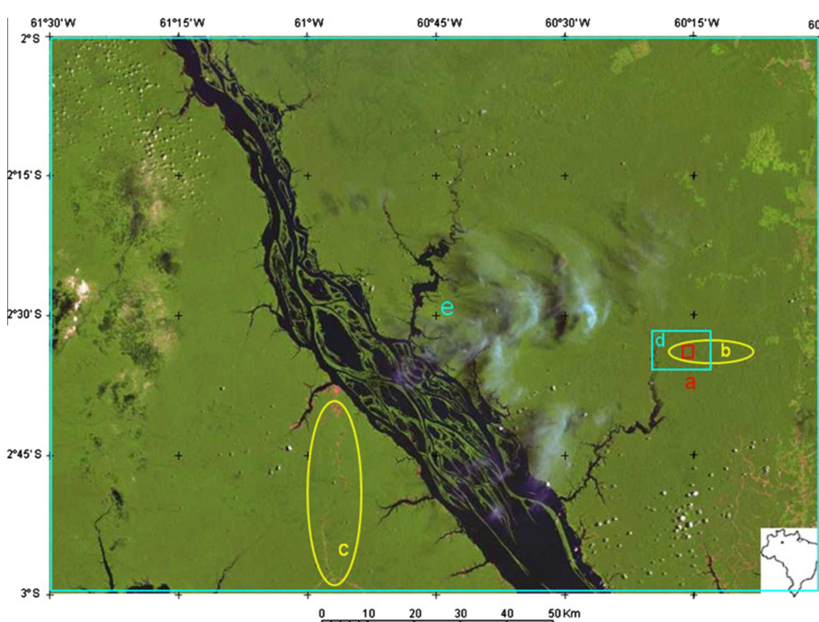

Fig. 4. HAND study area in the lower Rio Negro, NW of Manaus. Red square (a) depicts the calibration zone at the Igarapé Asu instrumented watershed (13.1 km^2). Yellow ellipses depict validation zones at the (b) Cuieiras and Tarumã catchments and in the (c) Novo Airão region. Blue rectangles indicate two larger scales of HAND mapping done for (d) the eastern Cuieiras catchment (519 km^2) and for (e) the lower Rio Negro catchment (18,553 km^2). Image Landsat TM 5, 4, 3 (RGB) September 1996. (For interpretation of the references to color in this figure legend, the reader is referred to the web version of this article.)

The Asu area lies within a terra firme terrain at the INPA Cuieiras reservation. Terra firme is generally defined as terrain not seasonally flooded by the Amazon main-stem flood wave (∼10 m). Canopy height varies from 20 to 35 m, with heterogeneous forests occurring on diverse terrain types. The landscape in and around the Asu catchment is composed mostly of plateaus (90–105 m asl) incised by a dense drainage network within broad swampy valleys (45–55 m asl). Dominant soil types in a typical catena along the hydrological transect are the clayey *latossolo amarelo álico* (typic Haplorthox or Acrorthox) on the plateaus, transitioning to less clayey *Argissolos Vermelho Amarelo álicos* (Orthoxic Tropohumult or Palehumult) on the slopes and ending with the sandy *Podzóis Hidromórficos* (Tropohumods–Troporthods) on the valley bottoms. A detailed description of this site can be found in Araujo et al. (2002), Waterloo et al. (2006), Cuartas et al. (2007) and Tomasella et al. (2008). Landscape and vegetation of the Igarapé Asu watershed are representative of the larger validation area and of other extensive areas in Amazonia.

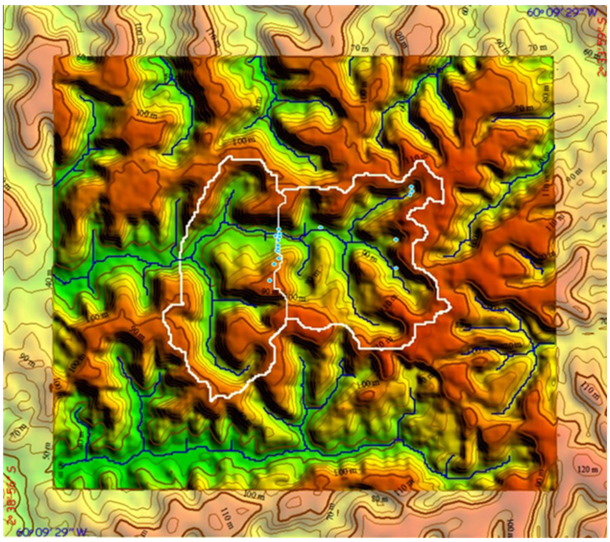

Fig. 5. The Asu instrumented watershed lies on terra firme tertiary terrain. Second- and third-order catchments of 6.5 km^2 and 13.1 km^2, respectively, are shown in the white outline. Average rainfall in the area is 2400 mm/year, and the accumulated area for the initiation site of perennial surface runoff (stream headwater) was found to be 0.4 km^2 (a total of 50 90-m SRTM-DEM pixels). The placement of the stream headwaters in the DEM, which determines the representation of drainage density, a key parameter in the HAND terrain normalization, was made based on field verification for all streams within the watershed and several outside it. The boundary between the second- and third-order catchments indicates the position of the hill slope hydrological transect. Blue dots indicate position of long-term water table monitoring wells (27 in total).

To acquire field data for calibration, we visited 120 points in the Asu catchment (Fig. 6), and another 90 points were visited for validation in several catchments across the lower Rio Negro region. Stream heads locations were also logged for verification of the calculated drainage network. Forest understory geo positioning (30-m horizontal accuracy) was done with a 12-channel GPS (Garmin GPSMAP 60CSx). Contrasting non-floodable local environments were identified in the field through hydrological data and cues in the topography, vegetation and soils. Soil types were identified by augering. Water table depth in the Asu catchment was obtained from an irregular sampling network of 27 piezometers installed in the valleys, major stream heads, and along the hill slope of the hydrological transect. At validation sites, the water table position criteria (surface, shallow or deep) was inferred from superficial soil saturation levels and the relative position in the local relief.

3.2. Defining soil environments

The hydrological transect (Fig. 6, site C1), running orthogonally from the second-order Asu stream to the top of the plateau (Fig. 7), represented all of the topographic features in the area, and contained the sampling points for vegetation, soil, soil–water and topography. Four broad and contrasting categories of terrain, or soil environments, were found for this catena: (a) near the stream, soils were *waterlogged*, meaning that the water table level is always at, or very close to, the surface, creating an almost permanent swamp; (b) moving away from the stream, the ground surface rises

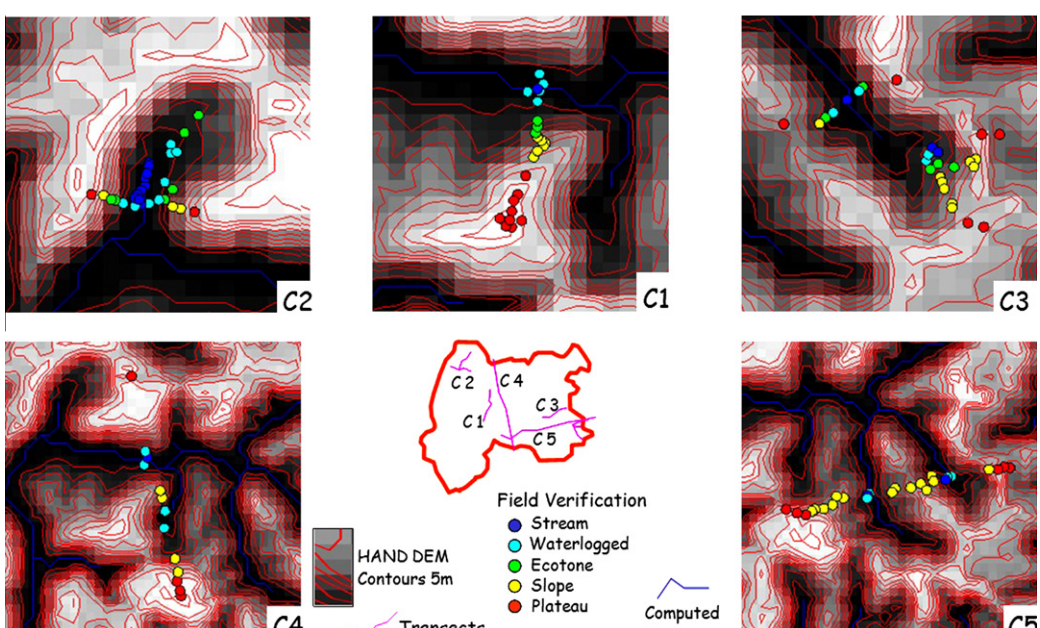

Fig. 6. Asu calibration area with the overlay of field verification points on the HAND model. Site C1 represents the hydrological transect; site C2 and C3 represent first order catchments; site C4 and C5 represent the north–south and east–west 2.5-km catchment crossing transects, respectively.

gently above the water table over a transition zone, or *ecotone*, where the vadose zone extends up to a depth of approximately 2 m; (c) further away from the stream, the landscape rises quickly, forming a steep *slope*, with the vadose layer becoming progressively dominant in the soil environment; (d) at the farthest distance from the stream, along the catchment divide, the landscape levels out into a *plateau*, with a vadose layer thicker than 30 m. The seasonal fluctuation of the water table alters the boundaries between zones (a and b) considerably, but not between zones (b and c).

3.3. Defining HAND classes

A HAND terrain class is here defined as a range of vertical distances to the nearest drainage reference level that bears roughly uniform hydrological relevance. We verified that the terrain variation within each class was considerably smaller than the variation found between contrasting classes.

3.3.1. Calibrating HAND classes

The calibration of HAND classes consisted of matching field-verified environment types with the corresponding distribution of heights in the HAND model (Fig. 8). The height distribution for the field verification points in the Asu catchment indicates that the normalized relative gravitational potential in the HAND model is an effective topographical parameter in the separation of local environments, especially for *waterlogged* from *ecotone* and upland classes. Taking these findings and other extensive field experience into account, HAND values of 5 m and 15 m were selected as preliminary best-guess thresholds between the three classes. To optimize this separation (lessen errors in class inclusion), we applied the simplex algorithm (Cormen et al., 2001), finding 5.3 m and 15.0 m as the best thresholds for the set of points available from

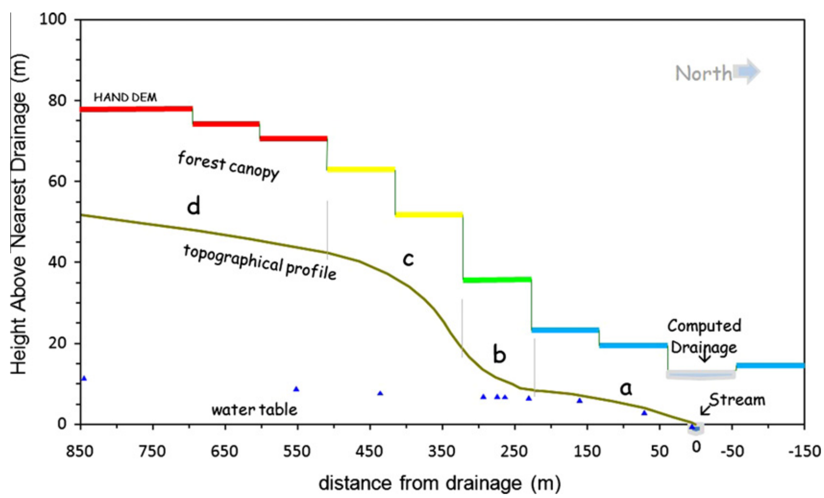

Fig. 7. Correspondence of local topography/groundwater with estimated classes of HAND model for Asu site C1. The topographic profile represents a typical hill slope for the region, encompassing all terrain types found in the study area. The long-term average water table depth is shown for each monitoring well along the hydrological transect (triangles; average position from 6 years of data). Verified soil environments are (a) *waterlogged*; (b) *ecotone*; (c) *slope*; and (d) *plateau*. The stepped profile, running on the top of the forest canopy, represents the HAND model topology (each step corresponding to a 90-m SRTM pixel) with the correspondence of estimated matching classes to soil environments represented in colors. The computed drainage occupies the lowest topographical height in the HAND model.

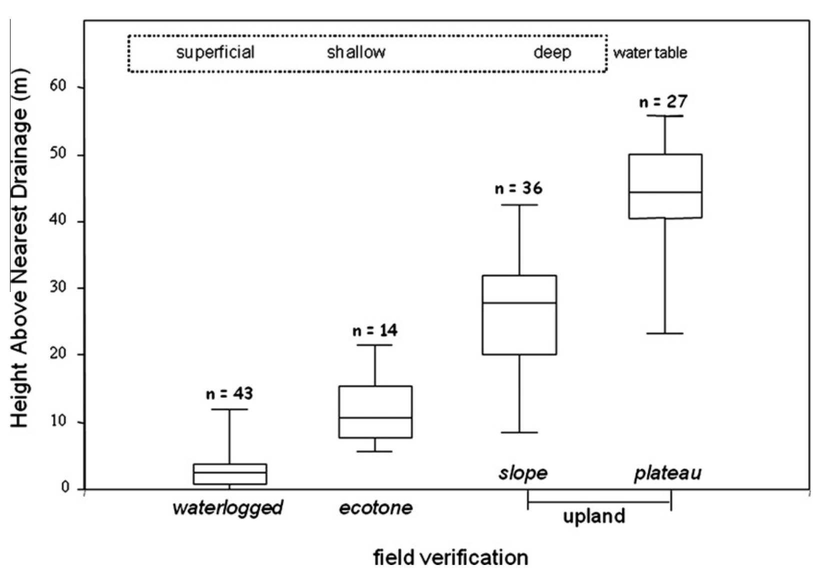

Fig. 8. Box-plot distributions of heights above the nearest drainage for the four field-identified distinct environments (modified from Rennó et al., 2008).

field verification. However, because the SRTM height data only resolves down to 1 m, the classes can be rounded to the nearest integer.

3.3.2. An auxiliary class

Although the upland class, which encompasses both flat and sloping terrain (*plateau* and *slope*), represented well the soil water condition (well drained, relatively deep water table) and in a relatively homogeneous way in comparison to the other two lowland classes, there are quite significant and distinct hydrological behaviors that set slopes and plateaus apart. Because the obvious separation between slope and plateau is slope angle, we analyzed the relationship between slope angle and the height above the nearest drainage for all four classes (Fig. 9).

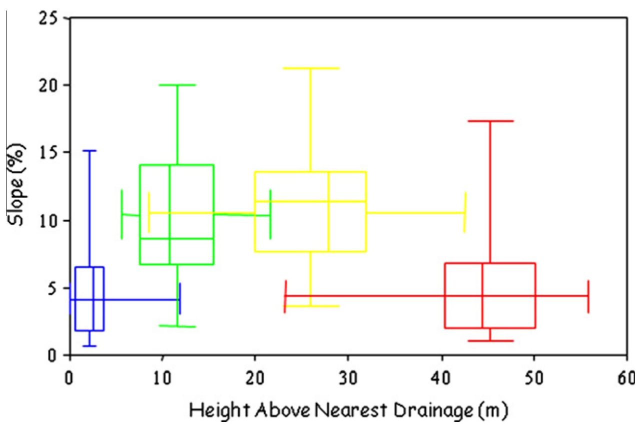

Fig. 9. Box-plot distributions of height above nearest drainage versus slope angle for the four field-identified environment classes (waterlogged – blue; ecotone – green; slope – yellow; plateau – red). (For interpretation of the references to color in this figure legend, the reader is referred to the web version of this article.)

The *waterlogged* and *plateau* classes share lower slope angles, and analogously, *ecotone* and *slope* share higher slope angles. Thus, a slope parameter alone cannot separate *waterlogged* from *plateau* or *ecotone* from *slope*. Here slope angle will be an auxiliary independent separator applied exclusively for the *upland* HAND class. The upland class (HAND > 15.0 m) was split on the basis of slope, with the initial threshold value arbitrarily set at a 6.5% (or 3°) and then optimized with the simplex algorithm resulting in a threshold value of 7.6%.

3.3.3. Calibration results

Using these field-optimized thresholds, we classified the HAND model into four classes. The field verification survey was accurate in identifying the local soil environment for each chosen point. Overlaying the field verification points onto the HAND classes (Fig. 10) reveals how well the HAND classification fared. For most points, the matching between field environments with HAND-predicted environments was good. This comparison suggests a coherent matching between field-identified local environments, corroborated by groundwater data, with the classified HAND topology. Nevertheless, unavoidable localization errors were responsible for a few mismatches. A few extreme values were found to overlap between classes, but the main reason for this is similar to that found in the calibration process at the hydrological transect: field verification data have a location accuracy of 30 m (GPS), whereas the SRTM data provide an average height for a 90 m pixel. Also, the spatial resolution and sampling density of field verification points is higher than the SRTM-DEM resolution. Another issue is the transition of environments, the foot of the slope for example, which occurred in a narrow band captured by the fine resolution of the field verification, but which could not be observed from the coarser DEM. Misplacement of classes in this case is much more an effect of resolution mismatch than an actual error of classification. However, because no systematic error favoring any HAND class was detected, we are confident for this

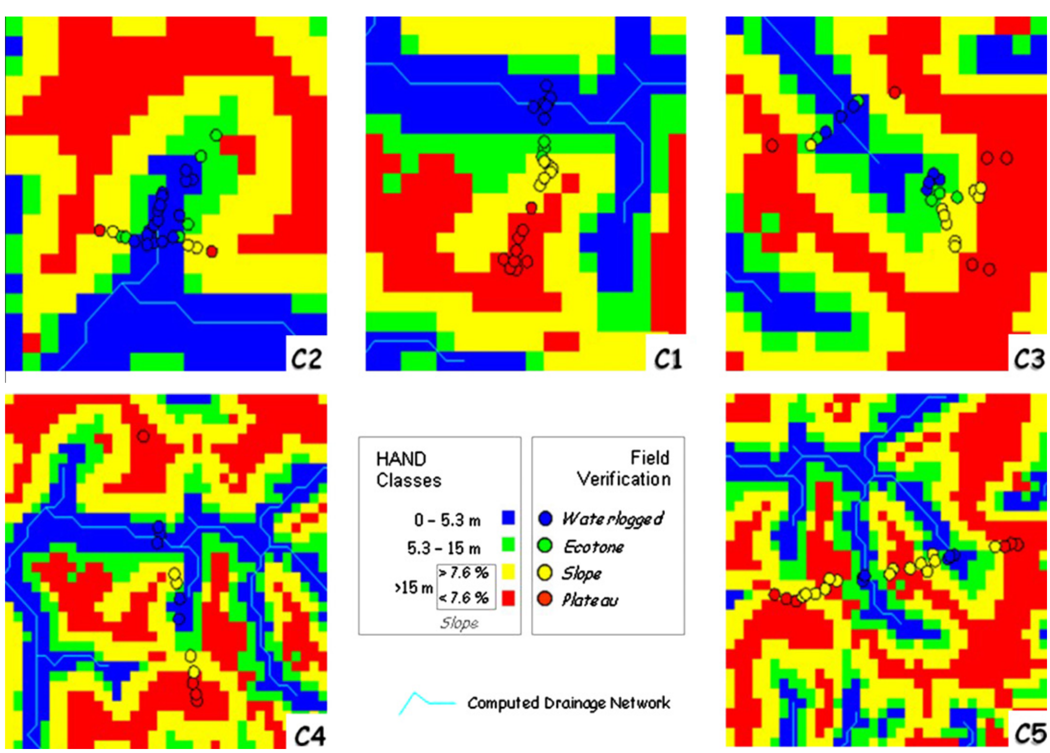

Fig. 10. Asu calibration study area with the overlay of field verification points on the classified HAND model. Matching colors between circles and underneath square pixels indicate good adjustment between field classes and HAND classes, respectively.

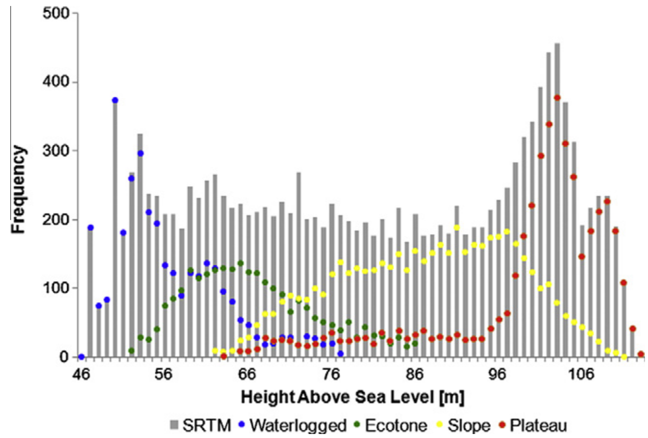

Fig. 11. Frequency distribution of heights above sea level in the SRTM-DEM for the Asu catchment overlaid by the frequency distributions for *height above sea level* of the four HAND classes.

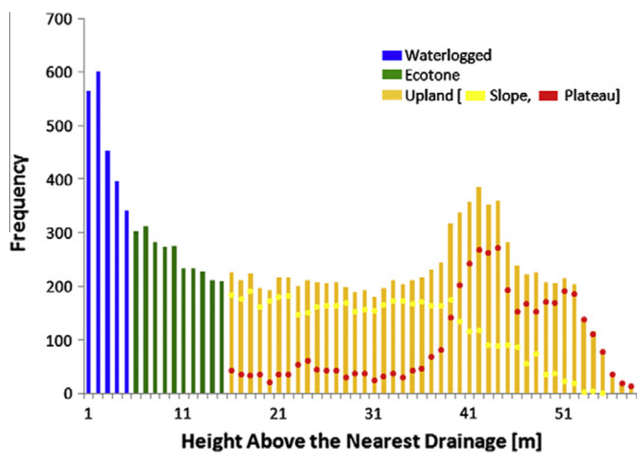

Fig. 12. Frequency distribution of heights above nearest drainage in the HAND model for the Asu catchment.

study that the area estimates for the local environments are sufficiently accurate.

3.4. Height frequency histograms

The third-order Asu catchment shows a multimodal frequency distribution for SRTM-DEM elevations (Fig. 11), with the heterogeneous distributions indicating actual topography. Height above sea level frequency distributions for the HAND classes were computed by overlaying the spatial masks for each HAND class (normalized) onto the SRTM-DEM (non-normalized). The overlap of elevations of the four contrasting environments, when seen on the actual topography, explains why height above sea level is unable to discriminate local environments properly. A bimodal frequency distribution for HAND model heights (Fig. 12) is evident for the same third-order Asu catchment, with the homogeneous distributions of heights indicating the normalization effect on topography. This analysis reveals that the normalized relative gravitational potential in the HAND model is a good parameter for the definition of relevant and distinct classes of stationary soil water conditions. The non-overlap of contrasting environments in the HAND topology indicates that the HAND classes are able to discriminate local environments properly.

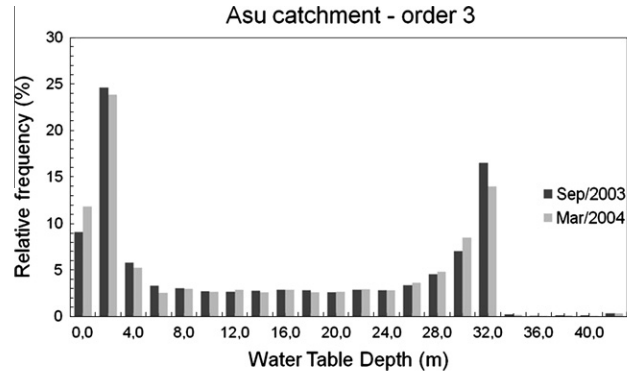

Fig. 13. Relative frequency distribution of water table depth for the third-order Asu catchment.

3.5. HAND and the water table

The topology of the water table can often mimic topography (Haitjema and Mitchell-Bruker, 2005), which seems to be the case for the second-order Asu catchment. The correlation of water table depths (long-term data from 27 piezometers) with HAND model heights ($y = 0.658x - 2.89$ $R^2 = 0.806$) indicates that the water table follows local normalized topography well. In this low order catchment, with relatively low relief, there is also a correlation with SRTM-DEM ($y = 0.561x - 31.41$ $R^2 = 0.674$), but if a more mountainous or larger area had been used for this analysis, then the correlation with SRTM-DEM elevations would degrade until becoming irrelevant because, on a larger scale, the depth of the water table is not controlled by height above sea level. To probe the relationship of water table depth with HAND heights beyond the low-density sampling of the piezometer network, we employed a simulated water table generated by Cuartas et al. using the DHSVM hydrological model (in preparation). The model was calibrated and validated for soil moisture (neutron probe), water table depth (piezometers) and stream flow discharge (Doppler profilers). Fig. 13 shows the frequency distribution of the simulated water table depth for two dates during the dry (September/2003) and wet season (March/2004). The distributions are bi-modal, as is the frequency distribution of height above nearest drainage in the HAND model (Fig. 12).

4. Validation

To test the robustness of the calibrated HAND classes (i.e., the ability to fit landform patterns with soil water conditions for ungauged catchments) we validated it for distinct terrains. For this study the chosen validation sites fell on similar geology (*Alter-do-Chão* formation) but with contrasting geomorphology between areas both close to (within a 12 km radius) and more distant (within a 120 km radius of the Asu catchment). The landscape type of the Igarapé Asu area, with a wide valley and relatively flat terrain, was the most representative case (absence of steep sided, deep valleys where plateau pixels would edge directly onto drainage pixels) for validation in this study. We used 70 validation points that fell in this category. The quantitative analysis (Fig. 14) showed a satisfactorily good validation for the three HAND classes, considering the same class thresholds adjusted in the calibration. This finding indicates that the classified HAND model is able to remotely estimate local environments from SRTM-DEM data with good confidence.

4.1. Large-scale validation through mapping

Mapping terrain using field surveying and point sampling has proved to be an unsatisfactory method to characterize landscape

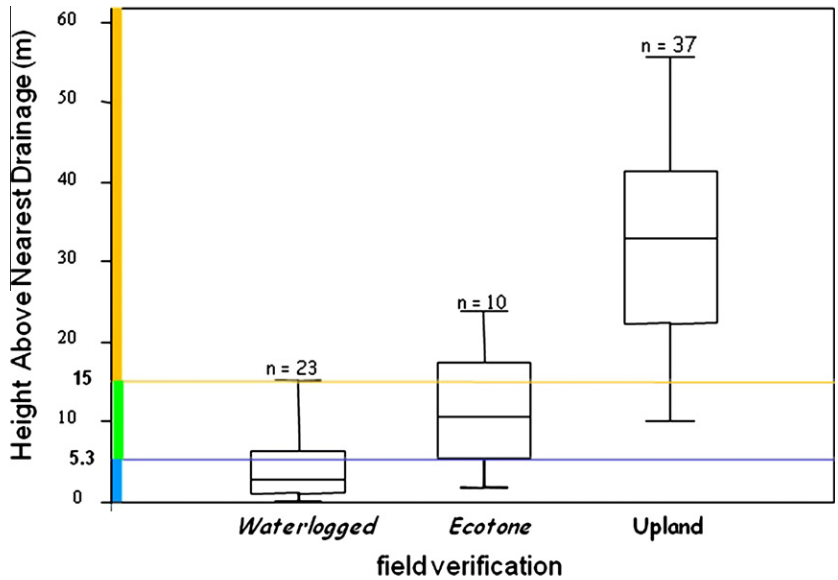

Fig. 14. HAND class validation: box-plot distributions of heights above the nearest drainage for the three field-identified distinct classes of environments. Validation points were all acquired outside the Asu calibration area.

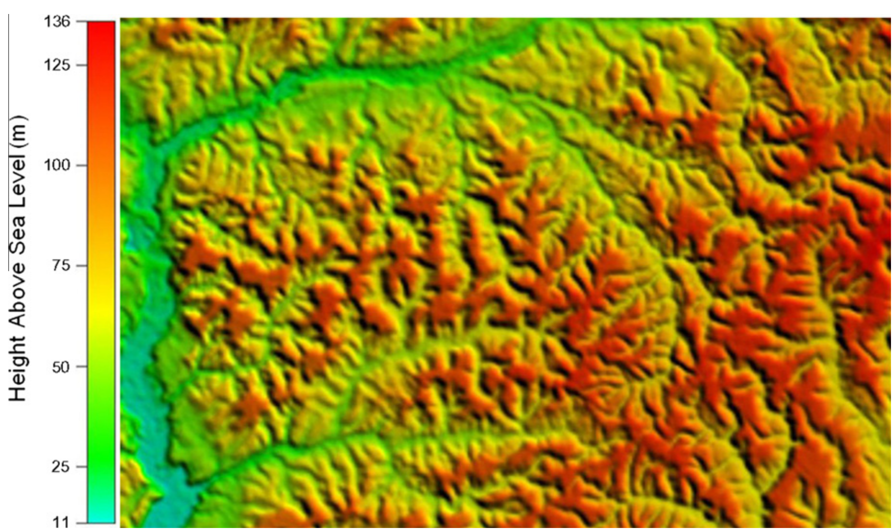

Fig. 15. SRTM-DEM color-shaded relief of the eastern Cuieiras catchment (horizontal resolution of 3′ ~90 m; vertical resolution, 1 m). Note sloping in the drainage network towards the SW. (For interpretation of the references to color in this figure legend, the reader is referred to the web version of this article.)

in a quantitative, functional and extensive manner (Crow et al., 2005; Vereecken et al., 2007). As a result, descriptive, observational or landscape-based modeling studies do not employ quantitative terrain maps as effectively as they could. The SRTM and other sources have produced detailed and extensive digital elevation data for all continents. We have applied the classified HAND model using such elevation data for mapping forested areas of central Amazonia, analyzing its capacity to map soil water environments beyond the local scale of the Asu calibration, at two additional scales.

4.1.1. 500 km^2

In the Cuieiras river catchment, which includes the HAND study area, the SRTM DEM (Fig. 15) shows major plateaus and etched valleys, also exhibiting the sea-ward topographical gradient across the area. Although it shows many features, such a DEM can only be used quantitatively for geomorphic studies. Soil types, water conditions and landscape processes can only be assessed quantitatively through laborious field surveys and local sampling, the larger-scale extrapolation from which are fraught with errors.

The normalized HAND model of the same area (Fig. 16) shows significant changes with respect to the drainage. Lowlands appear similar, with heights fluctuating close to the ground reference level of the drainage network, but it becomes apparent that the topographic gradient towards the sea is entirely missing. The hills bear similarity with the original DEM only within individual overland flow paths. Because drainage has been flattened out, successive flow paths converging along the drainage have now been repositioned vertically, resulting in a deformation of higher relief areas. On the plateaus the flat surfaces of the original DEM have been sculpted into various shapes, reflecting the coherence of basins, their divides and the effects of nearest drainages on the relative positions of flow paths.

The HAND model creates hydrological/terrain homogeneity within and with the drainage network, but it still lacks a useful quantitative description of the landscape. Classifying the HAND

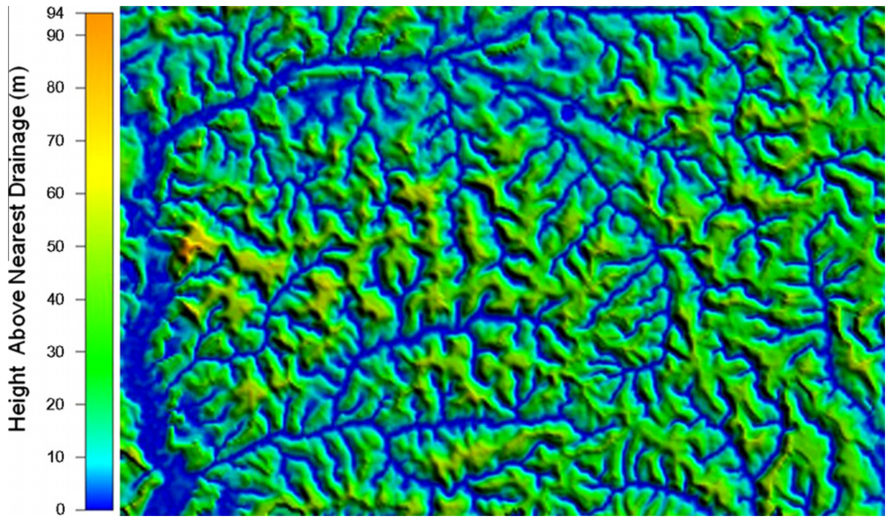

Fig. 16. HAND-DEM color-shaded relief of the eastern Cuieiras catchment computed from the SRTM-DEM (same resolution as source SRTM topography) showing drainage-normalized topography. Note that the drainage network is flattened and the geometries of hills have changed in some places. (For interpretation of the references to color in this figure legend, the reader is referred to the web version of this article.)

model into classes produces a map of terrain/hydrological character that can be used as an accurate and quantitative data source for landscape studies (Fig. 17).

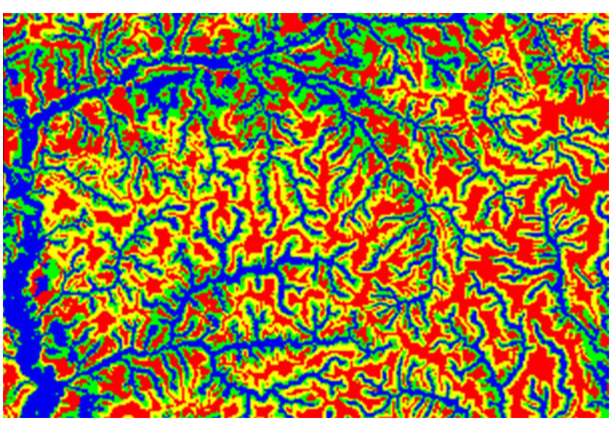

Fig. 17. HAND map of environments for the eastern Cuieiras catchment produced by dividing the HAND model according to field-verified classes.

Fig. 18 shows the frequency histogram of SRTM-DEM elevations and height above sea level of HAND classes for the larger Cuieiras area, computed in the same way as for the Asu area. In the frequency histogram of HAND model (Fig. 19), the classes are again completely separated, but in this case the distribution has a right skewed frequency curve (positive skew). This shape confirms that the lowland areas form an increasing large proportion of the area with increasing size of the basin, while there is a decrease in the proportion of slopes.

Besides the geographical location given by the HAND classes map, the respective areas occupied by the terrain types or distinctive soil–water environments can now be accurately accounted for (Table 1). In this terra firme area, it is striking to find that almost half of that terrain consists of lowland (43.1%) characterized by swamps and poorly drained soils.

4.1.2. 18,000 km^2

The green forest carpet, as seen in LANDSAT image of the Rio Negro study (Fig. 4), falsely suggests a monotonous terrain. The SRTM-DEM relief for the same area (Fig. 20) shows rich regional topographical features that are not visible in passive optical imagery. Topographical sea-bearing gradients can also be seen, with higher plateaus to the NE. However, little terrain/soil–water

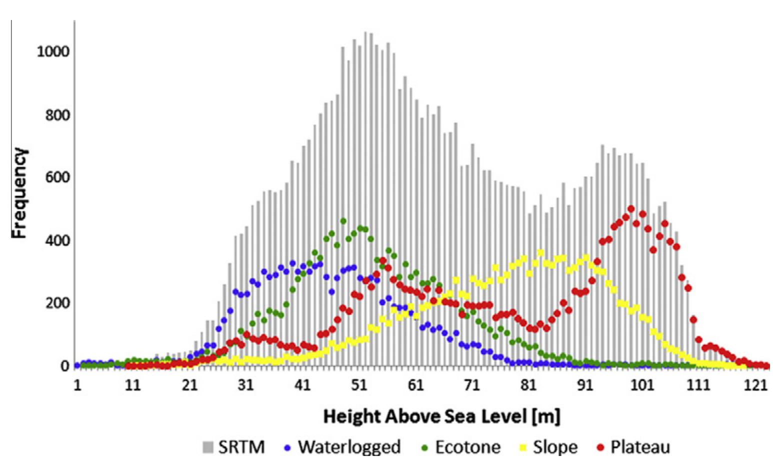

Fig. 18. Frequency distribution of heights above sea level in the SRTM-DEM for the eastern Cuieiras area.

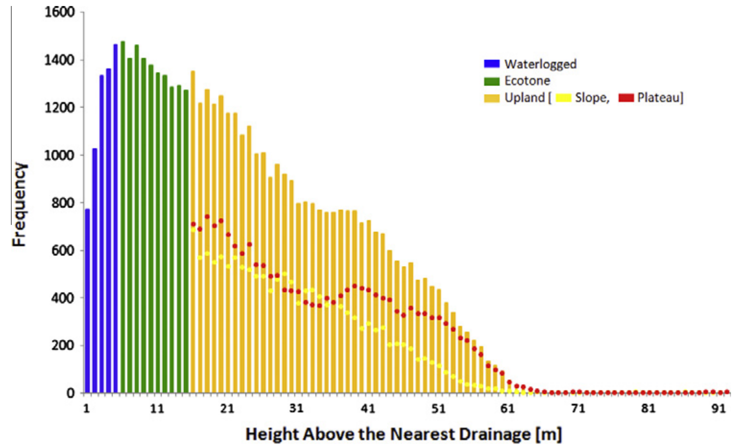

Fig. 19. Frequency distribution of heights above nearest drainage in the HAND model for the eastern Cuieiras area. (upland = slope + plateau).

Table 1
Breakdown of areas of the four-class HAND map for the eastern Cuieiras.

Class	Area (km^2)	% Area terra-firme	% Area terra-firme, grouped
Waterlogged	102.4	19.7	Lowland
Ecotone	121.2	23.4	43.1
Slope	159.2	30.7	Upland
Plateau	135.9	26.2	56.9
Total	518.7	100	100

quantitative information can be extracted from these data other than similarity of the geomorphic features.

For testing the HAND model on this much larger area (Fig. 21), we analyzed only terra firme landscape, masking out all floodable areas (igapós) using the JERS-1 floodland map (Mellack and Hess, 2004). The HAND model runs at the same resolution as the source DEM, and the size of the area to be computed is only limited by computer power.

The classified HAND model reveals an extraordinary richness of local environments (Fig. 22). Features that could not be seen in the HAND model alone become apparent, such as the areal extension of particular terrains or mosaic combinations of local environments and even signs of geomorphologic evolution. Variations in the *slope* and *plateau* classes on the opposite banks of the large river reveal interesting patterns. Each of these HAND classes could be further split or aggregated into different classes for different applications. For example, *plateau* could be grouped according to height asl extracted from the original SRTM-DEM, indicating coherent surfaces or distinctive vadose zone thickness. *Slope* could be split into lower slope, where tree roots can reach the water table, and upper slope, where distance to the water table make trees susceptible to drought caused by climate anomalies, such as El Niño. The areal breakdown into the four-class HAND model reveals that in the non-floodable part of the study area, or the terra firme, the swampy and poorly drained lowland terrain occupies an area larger (58.5%) than the well-drained upland terrain (41.5%) (Table 2). It has been assumed that terra firme is entirely upland (well drained soils), but becomes very clear with this analysis that terra firme includes vast areas of swampy lowlands whose importance cannot be ignored.

Fig. 23 shows the frequency histogram of SRTM–DEM elevations and height above sea level of HAND classes for the Rio Negro area computed in the same way as for the Asu area. At this larger scale, the overlap of environments remains evident.

In the frequency histogram of the HAND model (Fig. 24), the classes are again completely separated. The HAND histograms for the three areas indicate that the larger the area considered, the smoother the distribution.

The HAND model, calibrated using data from the Asu catchment, revealed good correlations between local environments

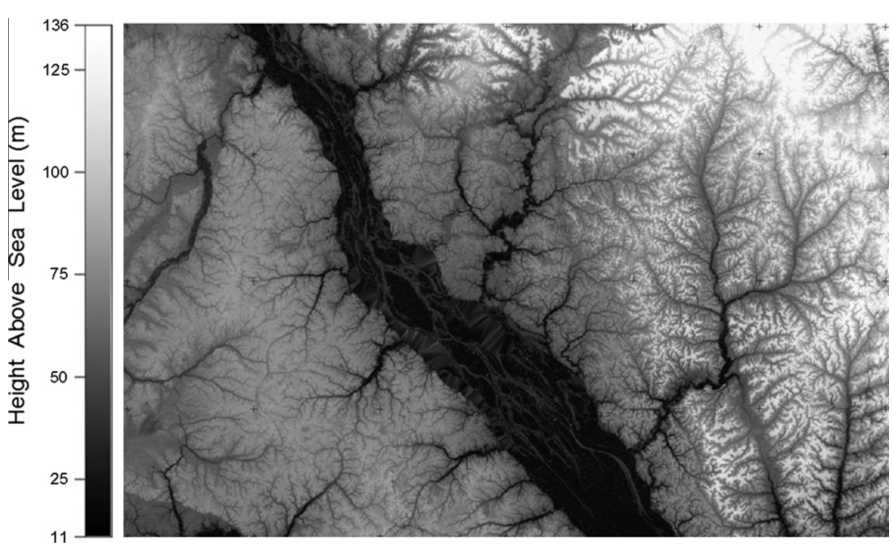

Fig. 20. SRTM-DEM shaded relief of the larger study area in the lower Rio Negro catchment showing rich details in the forest topography. Note higher hills in the NE.

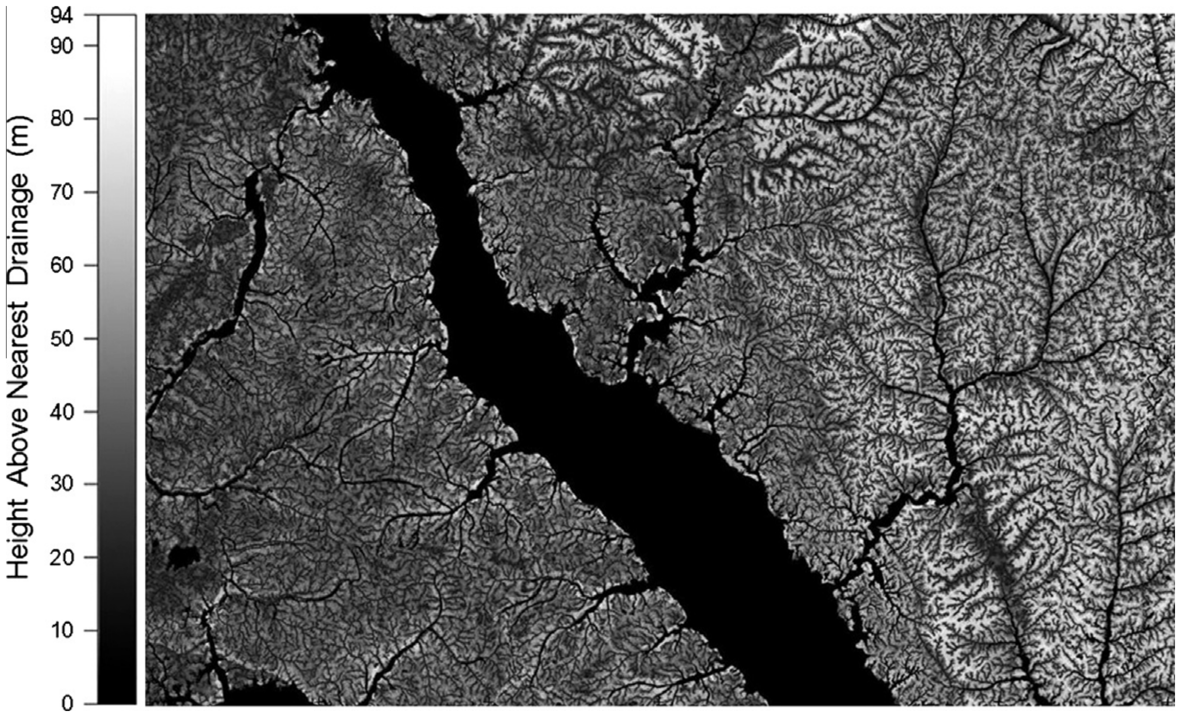

Fig. 21. HAND model shaded relief of the lower Rio Negro catchment computed from the SRTM-DEM showing drainage-normalized topography. Seasonal flood lands were removed from the analysis by a mask in black made using JERS-1 L band data (Mellack and Hess, 2004).

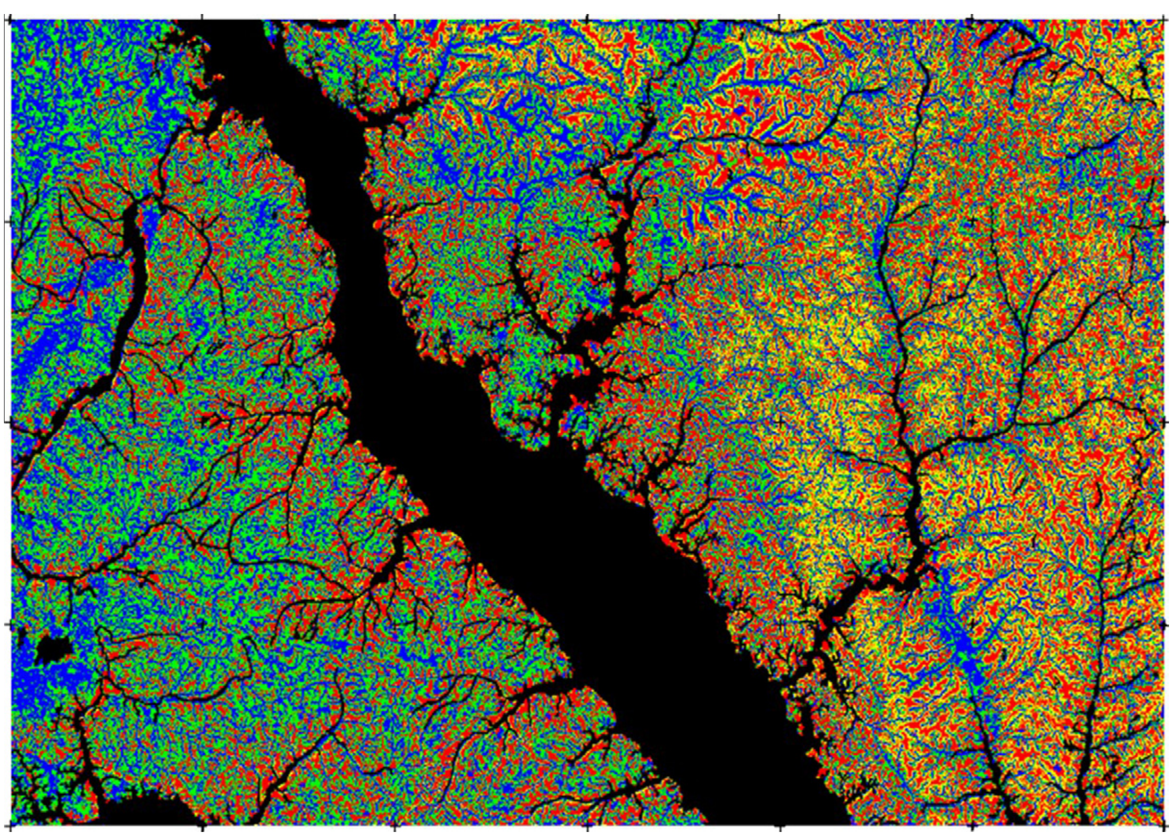

Fig. 22. HAND map of environments for the lower Rio Negro area produced by dividing the HAND model according to field-verified classes (lowlands in blue, waterlogged and green, ecotone; upland in yellow, slope and red, plateau). Note the very distinctive terrain features on different sides of the Rio Negro. (For interpretation of the references to color in this figure legend, the reader is referred to the web version of this article.)

and HAND classes and has been demonstrated to be robust during validation for the encompassing larger region. Additional and preliminary validation made in remote areas of Brazil (São Gabriel da Cachoeira, Balbina and Urucú in Amazonas State; eastern São Paulo

Table 2
Breakdown of areas for the four-class HAND map for the lower Rio Negro (terra-firme = total area − flood land).

Class	Area (km^2)	% of Area	% Area terra firme	% Area terra firme, grouped
Floodland (mask)	3386.4	18.3		
Waterlogged	3886.2	20.9	25.6	Lowland
Ecotone	4986.8	26.9	32.9	58.5
Slope	1689.0	9.1	11.1	Upland
Plateau	4605.1	24.8	30.4	41.5
Total	18,553.3	100	100	100

State; Rio de Janeiro State; and independently by Collischonn (2009) at the upper Tapajós river in Pará State and Grande Sertão Veredas in Minas Gerais State) has further corroborated the ability of the HAND model to remotely predict local saturated areas of ungauged catchments, irrespective of quite contrasting associations of geomorphology, soils and vegetation.

4.2. HAND vs. TWI

We tested the similarity between HAND heights and the TWI for the entire dataset encompassing our Rio Negro study area (excluding drainage cells and cells neighboring the divide), finding no significant correlation between the two variables (Fig. 25). Because the HAND variable is an explicit measure of the main physical feature linking terrain with water relative potential energy, the lack of correlation with TWI demonstrates that the latter is not a good descriptor of local draining potential.

5. Discussion

5.1. HAND fundamentals

The initial basis for the HAND model came from the definition of a drainage channel: perennial streamflows occur at the surface, where the soil substrate is permanently saturated. It follows that the terrain at and around a flowing stream must be permanently saturated, *independently of the height above sea level where the considered channel occurs*. Streamflows indicate the localized occurrence across the landscape of homogeneously saturated soils. The second basis for the HAND model came from the distinctive physical features of water circulation. Land flows proceed from the land to the sea in two phases: in *restrained flows* at the hillslope surface and subsurface; and in *freer flows* (or discharge) along defined natural channels. From these bases emerged the main question guiding HAND model development: how would hillslope topographic gradients be comparable among distinct flowpaths if local gradients along flowpaths (on hillslopes) could be teased apart and isolated from landscape-scale sea-ward gradients (in channels)?

The HAND model was structured using a few fundamental tenets of hydrology: the landform conditions the runoff trajectories (flowpaths) and, consequently, defines hydrologically consistent topological domains (catchments). Flowpaths define hydrological relationships between different points within a catchment,

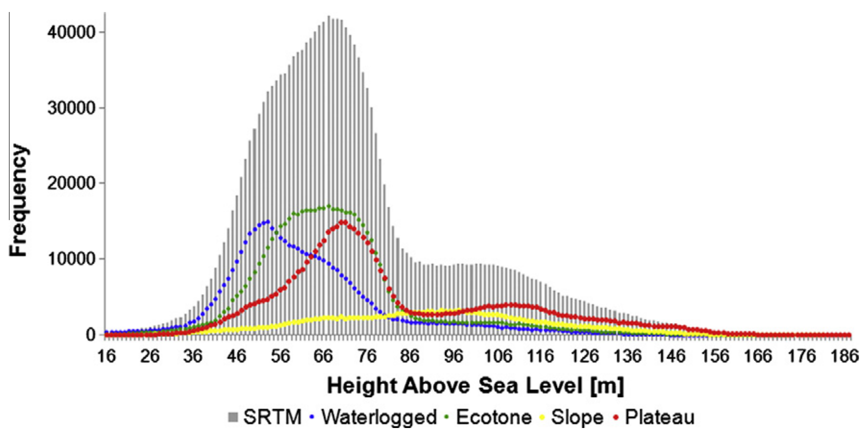

Fig. 23. Frequency distributions of heights above sea level for the SRTM-DEM, lower Rio Negro area.

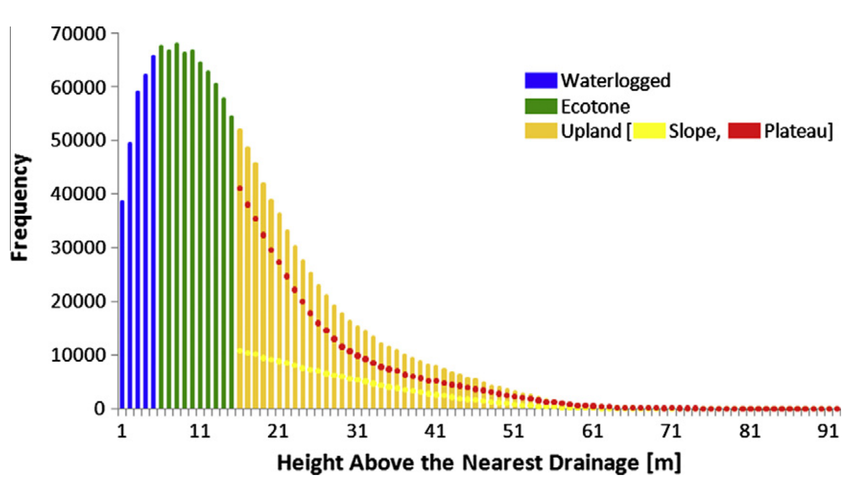

Fig. 24. Frequency distribution of heights above nearest drainage for the HAND model, lower Rio Negro area. (upland = slope + plateau).

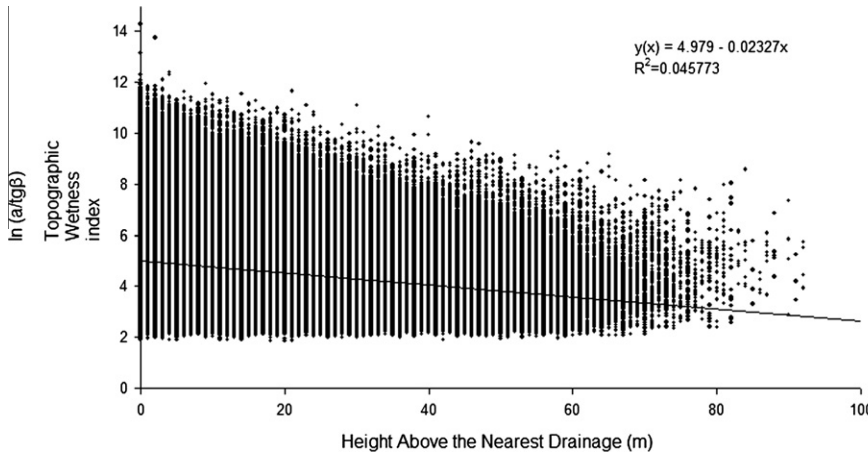

Fig. 25. Correlation between HAND heights with the topographical wetness index for the Rio Negro larger study area. (n = 1756887).

forming a hierarchical network. The accumulated area defines the upslope runoff-contributing surface at any given point along a flowpath, and the contributing area threshold defines the drainage network density (establishing the upper reach of perennial streamflows). Gravity then propels water down topographic gradients through the minimum energy trajectory (flowpath) moving from any point on and in the terrain towards the nearest point where it becomes a superficial drainage. These topological and physical principles establish functional spatial hierarchies that allow for a physically coherent separation of landscape-scale or drainage channel gradients (DCG) from hillslope flowpath gradients (HFG). It is important to distinguish between the DCG, with permanently (or seasonally) flowing streams – and the HFG – which may be subsurface or may only flow ephemerally as a result of large rainfall events. The HFG may also date back to a previous climate. In the HAND model, we fix DCG and normalize HFG with respect to DCG. The drainage network is used as a local frame of variable topographic reference such that the sea-ward gradients along channels are discarded, setting the drainage network as the lowest reference height in the new terrain model. Because each HFG outlet-to-the-drainage cell bears a different altitude asl, the leveling off of the drainage-channel in the HAND model implies bringing all of the catchment's HFG outlet cells to the same new drainage channel reference level. Then, the cells along each HFG are height normalized according to that reference level. The gravitational potential energy difference between any given cell along a HFG and the lowest extremity of the same flowpath at its stream outlet defines a stationary property of that cell, the relative gravitational potential, that we call *local draining potential*. The vertical distance (difference in level) of a given HFG cell to its drainage outlet cell is expressed as the absolute difference in height above sea level between those cells. Even though the HFG relative-heights in the HAND model lose their reference to sea level, they can uniquely identify the distributed local draining potentials, which are generalizable across the catchment and for different catchments. In a similar sense, the draining potential to a surface water outlet for the saturated ground water is known as hydraulic head (e.g. Vereecken et al., 2007). However, our use of the draining potential concept contrasts with downhill hydraulic gradients (Hjerdt et al., 2004) because we consider the topographic potential in height progression, meaning always starting at the drainage level (zero potential) and moving uphill along the HFGs towards the catchment divide (higher positive potentials). Draining potential also contrasts with drainage class, a common concept in pedology (e.g. Bell et al., 1992). While both concepts refer to stationary water properties of landscape, drainage class describes the water regimen only qualitatively, irrespective of associated energy potentials. Conversely, the HAND model heights univocally link the distributed draining potentials to their respective nearest drainages. Therefore, the molded surfaces of the HAND model are a *topology of local draining potentials*, which gives them relevant and practical hydrological meaning. The HAND model assumes that for each cell in the DEM, there must be a unique and topologically consistent HFG connecting that cell with its respective outlet to a stream. These connecting flowpaths bear all of the topological components that are extractable from a DEM, which allows for the spatially accurate normalization of local draining potentials.

5.2. Calibration and validation

Rigorously, the normalized topology of the HAND model is not directly about soil–water. The gravitational potential is a positional property of the landscape, a physical force that submits any water on and in the terrain to downward acceleration. Because under such force water infiltrates into the porous media (if it is not saturated) or moves downhill on the surface as runoff, draining to the stream, we equated the relative gravitational potential to a draining potential, that is, the net capacity for water to drain from its position on the hillslope to the nearest drainage channel. High HAND heights mean large draining potential, where water will drain effectively leading to the appearance of a vadose zone; low HAND heights mean low draining potential and proximity to the water table, where draining water will pool, creating waterlogging. The convincing association of terrain types with distinctive HAND height-classes made in the calibration, and widely corroborated by the validation, demonstrated that the relative gravitational potential in the HAND model has a very high correlation with soil–water saturation regimen. The depth of the saturated zone conditions superficial soil–water environments.

To generate the drainage network, a basis for the HAND model, channel initiation is the only deterministic threshold that needs to be addressed. We identified two factors as potential sources of uncertainty in the definition of accumulated area: automatic extraction from the DEM and hydrologic fluctuations. We examined the first factor in detail and found that for the verified accumulated area, the automatic extraction would miss stream headwaters by 1–2 SRTM-DEM pixels (less than 200 m), due to the masking of relief by the forest canopy. This effect was neither significant for the HAND model nor for the HAND classes, as the missed upper part of the stream had similar lowland terrain. For the same reason, high frequency fluctuations in the soil water condition should not influence significantly the HAND normalization and class allocation. Even for an oscillating headwater the only area theoretically affected in the HAND model calculations would be those relatively few flowpaths that gather to the fluctuating stretch of the stream head. From an exploratory analysis of the relationship between drainage density (defined by the contributing area threshold) and the HAND height histogram (Rennó et al., 2008), we found that the skewness in the HAND distribution of heights is directly proportional to the smoothness of the HAND model. Higher frequencies of the small HAND values, for example, result in a smoother topography of the HAND model, which implies a lower ability to distinguish and resolve contrasting local environments. If the calculated drainage network density remains within the range that realistically captures the Strahler order of the real drainage network, then the effect of slightly varying channel heads on the HAND model will not be significantly great.

Even though the soil–water calibration for the HAND classes was conducted in a small gauged catchment, the validation covered thousands of square kilometers of very heterogeneous terrain, all with ungauged catchments. The consistency of the HAND classes' thresholds for a variety of verified terrains, especially the 5 m indicating superficial saturation, was an extraordinary finding of this study. This suggests the importance of the local draining potential in shaping the soil–water saturation regimen, determining the depth of the water table. The non-arbitrary deterministic nature of these thresholds seems to be supported by a generalizable physical principle. It appears that such landscape-scale control of saturation regimen is the driving factor influencing vegetation cover, soil genesis and geomorphologic evolution. Correspondence of the HAND environments with landforms, landcover and other landscape characteristics, allows for the construction of a variety of HAND-based feature maps.

5.3. Relative topography

The quantitative association of local relative topography with soil water has been hinted at by a number of studies. Famiglietti et al. (1998) cited five studies, starting in 1959, that demonstrated that moisture content is inversely proportional to relative elevation. Crave and Gascuel-Odux (1997) pointed to a downslope topographic index (defined as the elevation difference between the considered point and the stream point corresponding to the outlet of the water pathway) as explaining well the temporal and spatial distribution of the surface water in a French catchment. Similarly, Qiu et al. (2001) found a significant correlation of the relative elevation (defined as the elevation difference between the sample point and the stream at the bottom of that hillslope) with layer-averaged and mean soil moisture for a catchment in China. In developing a generic computational procedure for segmenting landforms in Canada, MacMillan et al. (2000) applied two related relief descriptors, absolute height above the local pit cell and percent height relative to the nearest stream and divide. Thompson et al., in analyzing the distribution of hydromorphic soils (1997) and DEM resolution effects on attribute calculation and landscape modeling (2001), have quantified the significance of horizontal and vertical distances to the nearest depression. Bell et al. (1992, 1994) employed, among other variables, elevation above a local stream in the modeling of landscapes to map drainage classes. Kravchenko et al. (2002) found that horizontal distance to the drainage-way was useful to discriminate drainage classes. In developing logistic models to predict probabilities of soil drainage class occurrence, Campling et al. (2002) found that distance-to-the-river-channel was among the most important spatial determinants of class separation. All of these studies have directly or indirectly recognized the importance of relative local terrain distances as landscape variables influencing soil water dynamics. However, to our knowledge, no published work has set the stream channel as the base reference height against which all other flowpaths should be normalized. Provided that the stream network is well defined, the HAND model heights have uniform and universal hydrological significance.

5.4. Applications

The terrain normalization that we report here can be applied to DEMs of any terrain, generating HAND models with implicit geomorphologic, hydrological and ecological relevance. The significance of such terrain normalization for practical applications can be seen by calibrating HAND classes to match relevant soil water and land cover characteristics. The application of the HAND model provides the possibility of capturing and examining heterogeneities in local environments in a quantitative and widely comparable manner. Large-scale application of HAND maps in the accounting of environmental variables, many of which are very difficult to measure or model, promises significant advances in a number of disciplines. Soil and landscape modeling based on spatial information of terrain attributes (e.g. Moore et al., 1993, De Bruin and Stein, 1998) require environmentally relevant topography information for reaching their full quantitative and predictive potential. Thompson et al. (2001) listed three key factors for soil genesis/landscape modeling: representation of the continuous variability of soil properties across landscapes; relating of environmental factors to topography; and making spatial predictions of soil properties for unsampled locations. The HAND model offers spatially optimized and physically substantiated solutions for all three factors. Surface hydrology could benefit from the availability of soil parameter layers, which can be derived from accurately classified HAND models. In another study, we have successfully employed HAND-derived spatial soil and vegetation data in the parameterization of the DHSVM for an Asu catchment simulation (Cuartas et al., in preparation). Large-scale remote mapping of the soil moisture character, a crucial demand of advanced Earth System models (e.g. Koster et al., 2004), can be made feasible through the application of the HAND model to expansive areas without losing the information from low order catchments. In surface-atmosphere modeling, due to the large size of atmospheric grid cells, models cannot properly represent surface heterogeneities at finer scales. Using the HAND terrain maps, it will be possible to quantitatively scale up from real surface physical properties on a fine scale and avoid the guesswork of rough estimation that was previously involved in the empirical derivation of parameters (e.g. SIB, Sellers et al., 1986). Another critical area of application is in landscape hazards mapping and modeling, where assessment of risk zones is very complex and difficult (e.g. Bates and De Roo, 2000; van Westen et al., 2005). We have generated an original flood and landslide risk map for the São Paulo city metropolitan zone employing the HAND model (Nobre et al., 2010). Other HAND model applications could include proxy mapping of ecophysiology and evaporation. Similarly, biomass and nutrient dynamics could be landscape-integrated into realistic budgets. HAND terrain maps could also benefit the prediction of climate change scenarios and biome impacts, the modeling of land use, the analysis of buffer zones and conservation-strategies. The portfolio of applications for this new terrain model is likely to grow as different communities come to require knowledge of meaningful, contrasting and generalizable stationary hydrological properties of terrains at a fine local scale.

6. Conclusions

The height above the nearest drainage model is a drainage normalized version of a digital elevation model. The z axis variable of the HAND model is the normalized local height, defined as the vertical distance from a hillslope surface cell to a respective outlet-to-the-drainage cell, i.e., the difference in level between such cells that belong to a mutually connecting flowpath. The field testing of the HAND model, conducted in an instrumented hydrological catchment and on surrounding terrain in Amazonia, revealed strong and robust correlations between soil water conditions and the segmented classes in the HAND topology. This correlation is explained by the physical principle of the local gravitational potential, or relative vertical distance to the drainage, which we called local draining potential. Provided that the drainage network density is accurately represented in the HAND model, its representation of local soil draining potential is replicable for any type of terrain for which there is digital elevation data, irrespective of geology, geomorphology or soil complexities. The HAND model presents great applicability potential for a number of diverse subjects and disciplines, such as surface hydrology, meteorology, biogeochemistry, carbon cycling, biodiversity, conservation, land use and hazard risk assessment, and planning. Furthermore, the HAND model has the potential to become a good framework for the development of an objective, quantitative, systematic and universal way to classify and map terrain.

Acknowledgements

We especially thank Carlos Nobre and Paulo Nobre of INPE's Center for Earth System Sciences for their critical and precious support. We also thank Antonio Huxley for support in the field work and Evlyn Novo for the cession of the JERS-1 based flood land numerical mask. We thank Professor. H. Savenije and two anonymous reviewers for very positive insights. This work was developed with the support of the GEOMA modeling network (Brazil's Ministry of Science and Technology federal funding). The modeling work was partially supported by the FINEP/Rede Clima project (Grant 01.08.0405.01). The collaboration of the LBA project with the Asu instrumented catchment study was invaluable. The Asu field study was also supported by the PPG7/FINEP Ecocarbon project (Grant 64.00.0104.00) and European Commission DG-12 Science Carboncycle project.

References

Abbott, M.B., Bathurst, J.C., Cunge, J.A., O'Connell, P.E., Rasmussen, J., 1986. An introduction to the European hydrological system – Systeme Hydrologique Europeen (SHE). Journal of Hydrology 87, 45–59.

Araujo, A.C., Nobre, A.D., Kruijt, B., Elbers, J.A., Dallarosa, R., Stefani, P., Randow, C., Manzi, A.O., Culf, A.D., Gash, J.H.C., Valentini, R., Kabat, P., 2002. Comparative measurements of carbon dioxide fluxes from two nearby towers in a central amazonian rainforest: the manaus LBA site. Journal of Geophysical Research 107 (D20), 8090. doi:10.1029/2001JD000676.

Band, L.E., Moore, I.D., 1995. Scale: Landscape attributes and geographical information systems. Hydrological Processes 9 (3–4), 401–422.

Bates, P.D., De Roo, A.P.J., 2000. A simple raster-based model for flood inundation simulation. Journal of Hydrology 236 (1-2), 54–77.

Bell, J.C., Cunningham, R.L., Havens, M.W., 1992. Calibration and validation of a soil-landscape model for predicting soil drainage class. Soil Science Society of America Journal 56, 1860–1866.

Bell, J.C., Cunningham, R.L., Havens, M.W., 1994. Soil drainage class probability mapping using a soil-landscape model. Soil Science Society of America Journal 58, 464–470.

Beven, K., Calver, A., Morris, E.M., 1987. The institute of hydrology distributed model. Report 98, 1–26.

Beven, K.J., Kirkby, M.J., 1979. A physically based, variable contributing area model of basin hydrology. Hydrological Sciences Bulletin 24 (1), 43–69.

Beven, K.J., 1995. Linking parameters across scales: sub grid parameterizations and scale dependent hydrological models. Hydrological Processes 9 (5–6), 507–525.

Beven, K.J., 1996. A discussion of distributed hydrological modeling. In: Distributed Hydrological Modeling. Kluwer Academic Publishers, pp. 255–278, Chapter 13a.

Campling, P., Gobin, A., Feyen, J., 2002. Logistic modeling to spatially predict the probability of soil drainage classes. Soil Science Society of America Journal 66, 1390–1401.

Collischonn, W., 2009. Aplicação do descritor HAND para mapeamento de áreas saturadas. Apresentação no Primeiro Workshop do HAND, Centro para Ciência do Sistema Terrestre, INPE, São José dos Campos, Brazil.

Cormen, T.H., Leiserson, C.E., Rivest, R.L., Stein, C., 2001. The simplex algorithm. In: Introduction to Algorithms, second ed., MIT Press and McGraw-Hill, pp. 790–804. ISBN 0-262-03293-7, Section 29.3.

Crave, A., Gascuel-Odux, C., 1997. The influence of topography on time and space distribution of soil surface water content. Hydrological Processes 11, 203–210.

Crow, W.T., Bindlish, T., Jackson, T.J., 2005. The added value of spaceborn passive microwave soil moisture retrievals for forecasting rainfall–runoff partitioning. Geophysical Research Letters 32 (L18401). doi:10.1029/2005GL023543.

Cuartas, L.A., Tomasella, J., Nobre, A.D., Hodnett, M.G., Waterloo, M.J., Múnera, J.C., 2007. Interception water-partitioning dynamics for a pristine rainforest in Central Amazonia: marked differences between normal and dry years. Agricultural and Forest Meteorology 145 (1–2), 69–83.

Cuartas, L.A., Tomasella, J., Nobre, A.D., Nobre, C.A., Hodnett, M.G., Waterloo, M.J., de Oliveira, S.M., von Randow, R.C., Trancoso, R., Ferreira, M., in preparation. Distributed Hydrological modeling for a Micro-scale Rainforest Watershed in Amazonia: model evaluation and advances in calibration using the new HAND terrain model. Journal of Hydrology.

Curkendall, D.W., Fielding, E.J., Cheng, T.-H., Pohl, J.M., 2003. A computational-grid based system for continental drainage network extraction using SRTM digital elevation models. In: Proceedings of the HPSECA/IPCC Conference, Taiwan.

Dahl, M., Nilsson, B., Langhoff, J.H., Refsgaard, J.C., 2007. Review of classification systems and new multi-scale typology of groundwater–surface water interaction. Journal of Hydrology 344 (1–2), 1–16.

De Bruin, S., Stein, A., 1998. Soil-landscape modeling using fuzzy c-means clustering attribute data derived from a digital elevation model _DEM. Geoderma 83, 17–33.

Deng, Y., 2007. New trends in digital terrain analysis: landform definition, representation, and classification. Progress in Physical Geography 31, 405–419.

Entekhabi, D., Rodriguez-Iturbe, I., Castelli, F., 1996. Mutual interaction of soil moisture state and atmospheric processes. Journal of Hydrology 184, 3–17.

Famiglietti, J.S., Rudnicki, J.W., Rodell, M., 1998. Variability in surface moisture content along a hillslope transect: Rattlesnake Hill, Texas. Journal of Hydrology 210, 259–281.

Flügel, W.A., 1995. Delineating hydrological response units by geographical information system analyses for regional hydrological modeling using PRMS/MMS in the drainage basin of the River Bröl, Germany. Hydrological Processes 9 (3–4), 423–436.

Garbrecht, J., Martz, L.W., 1997. The assignment of drainage direction over flat surfaces in raster digital elevation models. Journal of Hydrology 193, 204–213.

Gessler, P.E., Chadwick, O.A., Chamran, F., Althouse, L., Holmes, K., 2000. Modeling soil–landscape and ecosystem properties using terrain attributes. Soil Science Society of America Journal 64, 2046–2056.

Grabs, T., Seibert, J., Bishop, K., Laudon, H., 2009. Modeling spatial patterns of saturated areas: a comparison of the topographic wetness index and a dynamic distributed model. Journal of Hydrology 373, 15–23.

Grimaldi, S., Nardi, F., Di Benedetto, F., Istanbulluoglu, E., Bras, R.L., 2007. A physically-based method for removing pits in digital elevation models. Advances in Water Resources 30, 2151–2158.

Haitjema, H.M., Mitchell-Bruker, S., 2005. Are water tables a subdued replica of the topography? Ground Water 43 (6), 781–786.

Hansen, M.K., Brown, D.J., Dennison, P.E., Graves, S.A., Bricklemyer, R.S., 2009. Inductively mapping expert-derived soil-landscape units within dambo wetland catenae using multispectral and topographic data. Geoderma 150 (1–2), 72–84.

Hjerdt, K.N., McDonnell, J.J., Seibert, J., Rodhe, A., 2004. A new topographic index to quantify downslope controls on local drainage. Water Resources Research 40, W05602.

Jenny, H., 1941. Factors of Soil Formation, A System of Quantitative Pedology, Republished in 1994, McGraw-Hill, 100pp.

Jenson, S.K., Domingue, J.O., 1988. Extracting topographic structure from digital elevation data for geographic information system analysis. Photogrammetric Engineering Remote Sensing 54 (11), 1593–1600.

Jones, R., 2002. Algorithms for using a DEM for mapping catchment areas of stream sediment samples. Computers & Geosciences 28, 1051–1060.

Kalma, J.D., Sivapalan, M. (Eds.), 1995. Scale Issues in Hydrological Modeling. John Wiley and Sons Inc., UK, 504 pp.

Koster, R.D., Dirmeyer, P.A., Guo, Z., Bonan, G., Chan, E., Cox, P., Gordon, C.T., Kanae, S., Kowalczyk, E., Lawrence, D., Liu, P., Lu, C.-H., Malyshev, S., McAvaney, B., Mitchell, K., Mocko, D., Oki, T., Oleson, K., Pitman, A., Sud, Y.C., Taylor, C.M., Verseghy, D., Vasic, R., Xue, Y., Yamada, T., 2004. Regions of strong coupling between soil moisture and precipitation. Science 305 (5687), 1138–1140.

Kravchenko, A.N., Bollero, G.A., Omonode, R.A., Bullock, D.G., 2002. Quantitative mapping of soil drainage classes using topographical data and soil electrical conductivity. Soil Science Society of America Journal 66, 235–243.

Lindsay, J.B., 2006. Sensitivity of channel mapping techniques to uncertainty in digital elevation data. International Journal of Geographical Information Science 20 (6), 669–692.

Lindsay, J.B., 2005. The terrain analysis system: a tool for hydro-geomorphic applications. Hydrological Processes 19, 1123–1130.

Lindsay, J.B., Creed, I.F., 2005. Removal of artifact depressions from digital elevation models: towards a minimum impact approach. Hydrological Processes 19, 3113–3126.

MacMillan, R.A., Pettapiece, W.W., Nolan, S.C., Goddard, T.W., 2000. A generic procedure for automatically segmenting landforms into landform elements using DEMs, heuristic rules and fuzzy logic. Fuzzy Sets and Systems 113 (1), 81–109.

Martz, L.W., Garbrecht, J., 1998. The treatment of flat areas and depressions in automated drainage analysis of raster digital elevation models. Hydrological Processes 12, 843–855.
Mellack, J.M., Hess, L.L., 2004. Remote sensing of wetlands on a global scale. SIL News 42, 1–5.
Miliaresis G., 2008. Quantification of terrain processes. Lecture notes in geoinformation & chartography, XIV, 13-28. [doi:10.1007/978-3-540-77800-4_2]. In: Advances in digital terrain analysis, Springer, Editors: Zhou, Q., Lees, B., Tang, G., ISBN 978-3-540-77799-1, 462 p.
Moore, I.D., Grayson, R.B., Ladson, A.R., 1992. Digital terrain modeling: a review of hydrological, geomorphological, and biological applications. Hydrological Processes 5 (1), 3–30.
Moore, I.D., Gessler, P.E., Nielsen, G.A., Peterson, G.A., 1993. Soil attribute prediction using terrain analysis. Soil Science Society of America Journal 57, 443–452.
Nardi, F., Grimaldi, S., Santini, M., Petroselli, A., Ubertini, L., 2008. Hydrogeomorphic properties of simulated drainage patterns using digital elevation models: the flat area issue. Hydrological Science Journal 53 (6), 1176–1193.
Nobre, C.A., Young, A.F., Saldiva, P., Marengo, J.A., Nobre, A.D., Alves Jr., S., Silva, G.C.M., Lombardo, M., 2010. Vulnerabilidades das Megacidades Brasileiras às Mudanças Climáticas: Região Metropolitana de São Paulo, Sumário Executivo. Embaixada Reino Unido, Rede Clima e Programa FAPESP em Mudanças Climáticas, 31pp.
O'Callaghan, J.F., Mark, D.M., 1984. The extraction of drainage networks from digital elevation data. Computer Vision, Graphics and Image Processing 28, 323–344.
O'Loughlin, E.M., 1986. Prediction of surface saturation zones in natural catchments by topographic analysis. Water Resources Research 22 (5), 794–804.
O'Loughlin, E.M., 1990. Modeling soil water status in complex terrain. Agricultural and Forest Meteorology 50 (1–2), 23–38.
Qiu, Y., Fu, B., Wang, J., Chen, L., 2001. Soil moisture variation in relation to topography and land use in a hillslope catchment of the Loess Plateau, China. Journal of Hydrology 240 (3–4), 243–263.
Rennó, C.D., Nobre, A.D., Cuartas, L.A., Soares, J.V., Hodnett, M.G., Tomasella, J., Waterloo, M., 2008. HAND, a new terrain descriptor using SRTM-DEM; mapping terra-firme rainforest environments in Amazonia. Remote Sensing of Environment 112, 3469–3481.
Rieger, W., 1998. A phenomenon-based approach to upslope contributing area and depressions in DEMs. Hydrological Processes 12, 857–872.
Rodriguez-Iturbe, I., 2000. Ecohydrology: a hydrologic perspective of climate-soil-vegetation dynamics. Water Resources Research 36 (1), 3–9.
Sellers, P.J., Mintz, Y., Sud, Y.C., Dalcher, A., 1986. A simple Biosphere Model (SIB) for use within general circulation models. Journal of Atmospheric Sciences 43 (6), 505–531.
Schaake, J.C., Koren, V.I., Duan, Q.Y., Mitchell, K., Chen, F., 1996. Simple water balance model for estimating runoff at different spatial and temporal scales. Journal of Geophysical Research 101 (D3), 7461–7475.
Sivapalan, M., Blöschl, G., Zhang, L., Veressy, R., 2003a. Downward approach to hydrological prediction. Hydrological Processes 17, 2101–2111.
Sivapalan, M., Takeuchi, K., Franks, V.K., Gupta, V.K., Karambiri, H., Lakshmi, V., Liang, X., McDonnell, J.J., Mendiondo, E.M., O'Connell, P.E., Oki, T., Pomeroy, J.W., Schertzer, Uhlenbrook, S., Zehe, E., 2003b. IAHS Decade on Predictions in Ungauged Basins (PUB), 2003–2012: shaping an exciting future for the hydrological sciences. Hydrological Sciences Journal 48 (6), 857–880.
Stieglitz, M., Rind, D., Famiglietti, J., Rosenzweig, C., 1997. An efficient approach to modeling the topographic control of surface hydrology for regional and global climate modeling. Journal of Climate 10, 118–137.
Sørensen, R., Zinko, U., Seibert, J., 2005. On the calculation of the topographic wetness index: evaluation of different methods based on field observations. Hydrology and Earth System Sciences Discussion 2, 1807–1834.
Tarboton, D.G., 1997. A new method for the determination of flow directions and contributing areas in grid digital elevation models. Water Resources Research 33 (2), 309–319.
Thompson, J.A., Bell, J.C., Butler, C.A., 1997. Quantitative soil-landscape modeling for estimating the areal extent of hydromorphic soils. Soil Science Society of America Journal 61, 971–980.
Thompson, J.A., Bell, J.C., Butler, C.A., 2001. Digital elevation model resolution: effects on terrain attribute calculation and quantitative soil-landscape modeling. Geoderma 100, 67–89.
Tomasella, J., Hodnett, M.G., Cuartas, L.A., Nobre, A.D., Waterloo, M.J., Oliveira, S.M., 2008. The water balance of an Amazonia micro-catchment: the effect of interannual variability of rainfall on hydrological behaviour. Hydrological Processes 22 (13), 2133–2147.
Turner, M.G., 1989. Landscape ecology: the effect of pattern on process. Annual Review of Ecology and Systematics 20, 171–197.
Vereecken, H., Kasteel, R., Vanderborght, J., Harter, T., 2007. Upscaling hydraulic properties and soil water flow processes in heterogeneous soils: a review. Vadose Zone Journal 6, 1–28.
Wagener, T., Wheater, H.S., Gupta, H.V., 2004. Rainfall–Runoff Modeling in Gauged and Ungauged Catchments. Imperial College Press, London.
Wagener, T., Wheater, H.S., 2006. Parameter estimation and regionalization for continuous rainfall-runoff models including uncertainty. Journal of Hydrology 320, 132–154.
Wang, J., Endreny, T.A., Hassett, J.M., 2005. A flexible modeling package for topographically based watershed hydrology. Journal of Hydrology 314, 78–91.
Waterloo, M.J., Oliveira, S.M., Drucker, D.P., Nobre, A.D., Cuartas, L.A., Hodnett, M.G., Wilma, I.L., Jans, W.P., Tomasella, J., Araujo, A.C., Pimentel, T.P., Munera Estrada, J.C., 2006. Export of organic carbon in run-off from an Amazonian rainforest black water catchment. Hydrological Processes 20, 2581–2597.
van Westen, C.J., Asch, T.W.J., Soeters, R., 2005. Landslide hazard and risk zonation: why is it still so difficult? Bulletin of Engineering Geology and the Environment 65 (2), 167–184.
Wigmosta, M.S., Vail, L.W., Lettenmaier, D.P., 1994. A distributed hydrology-vegetation model for complex terrain. Water Resources Research 30 (6), 1665–1679.
Wigmosta, M.S., Nussen, B., Storck, P., 2002. The distributed hydrology soil vegetation model. In: Singh, V.P., Frevert, D.K. (Eds.), Mathematical Models of Small Watershed Hydrology and Applications. Water Resources Publications LLC, pp. 7–42.